
2-2 Monitoring and Prediction of Geospace Environment

2-2-1 Monitoring and Forecasting of Geospace Disturbances, and its Importance

NAGATSUMA Tsutomu

Since human beings will expand their sphere of activity toward space environment, the space surrounding the Earth, which we call “geospace”, is the unavoidable region for us. In geospace, various disturbances occur due to solar and solar wind activity. These geospace disturbances could affect not only artificial satellites but also ground-based social infrastructures. Hence, it is important to monitor and predict such geospace disturbance. This paper introduces the ongoing approaches being taken at the National Institute of Information and Communications Technology (NICT) toward monitoring and forecasting of geospace disturbances.

Keywords

Geospace, Observation network, Disturbance, Monitoring, Prediction

1 Introduction

The earth is a planet with an intrinsic magnetic field. Plasma bulk flows from the Sun (solar wind) form a magnetosphere around the earth, within which a characteristic plasma region is shaped. In addition, the interaction between the solar wind and the magnetosphere induces various kinds of electromagnetic disturbances inside the magnetosphere (source: “Studies of Various Space Weather Phenomena”, “Special Issue on Space Weather Forecasting 1”, Journal of the Communications Research Laboratory, Vol. 49, No. 3, 2002). The term “space” broadly refers to all space external to the earth’s upper atmosphere and is associated in our minds with many different concepts. Therefore, the term is inappropriate in referring to the ionosphere and the magnetosphere. Instead, the term “geospace” has recently come into common use to describe the space surrounding the earth as a familiar

stage of human activity.

Variations in geospace environment (geospace disturbances) could immensely affect artificial satellite and astronauts working in space as well as ground-based social infrastructures. Space weather forecasting is essential for enhancing the security and safety of social infrastructures, such as telecommunications and broadcasting, and space activities. The monitoring and predicting geospace disturbances are parts of the essential role for space weather forecasting. This paper introduces the ongoing approaches being taken at the National Institute of Information and Communications Technology (NICT) toward monitoring and forecasting of geospace disturbances, and also discusses the significance thereof.

2 Effects of geospace disturbances

This chapter discusses how space weather disturbances occurring in geospace affect artificial satellites and ground-based social infrastructures. The effects of satellite navigation and positioning due to the variation of electron density in the ionosphere have already been discussed in another paper [1].

2.1 Variations in radiation belt particles

The magnetosphere contains a region called the radiation belt. The radiation belt is divided into an inner belt (mainly composed of high-energy protons) and an outer belt (primarily based on high-energy electrons). The high-energy electrons in the outer belt vary significantly under the influence of geomagnetic storms, the largest-scale disturbance phenomena occurring in geospace through interaction of the solar wind-magnetosphere-ionosphere compound system [2]. Once lost in the particle flux in the main phase of geomagnetic storms, electron flux in the outer radiation belt sometimes be regained upon acceleration and heating in the inner magnetosphere during the recovery phase of the storms. The high-energy electrons that comprise the bulk of the outer belt have energy of 1 MeV or higher and are known to penetrate the airframes of typical artificial satellites, thereby inducing deep internal dielectric charging. The occurrence of any consequential discharge could cause the malfunctioning of internal electronics and other electric circuit, leading to satellite failures or other problems. The successive failure of Canada's Anik1 and Anik2 communications satellites in January 1994 have been associated with internal discharges resulting from the flux enhancement of the relativistic electrons in the outer radiation belt [3].

2.2 Variations in substorm particles

Substorms are among the fundamental disturbance phenomena occurring in geospace through interaction of the solar wind-magne-

tosphere-ionosphere compound system. This phenomenon in which auroras suddenly breaks up in the midnight region of the aurora oval, and then expand to the north, south, east and west, results in auroras varying dynamically for 30 minutes to about two hours. Corresponding to this optical auroral activity, the current flowing through the ionosphere grows to cause sharp geomagnetic variations in the auroral regions. Substorms inject high-temperature plasma having energy on the order of several tens of keV inside the magnetosphere. Such high-temperature plasma arriving at geostationary orbit is known to induce a surface charge of an artificial satellite on the same orbit [4]. Once the satellite's surface becomes charged with high voltage, there is a greater risk of discharge that could interfere with satellite operations. The accident involving the ADEOS II satellite on October 25, 2003, might be caused by the satellite's surface material having been charged by auroral electrons that short-circuited its power cables [5]. Moreover, analyses presume that 54% of satellite failures have been caused by charging phenomena, including deep dielectric charging [6].

2.3 Geomagnetic variations

As explained in the previous sections, the current system in geospace is dynamically developed during substorms, geomagnetic storms, and other phenomena, and produces geomagnetic variations on the ground. Large magnetic field variations due to auroral activity observed particularly in the polar regions. If sharp geomagnetic variations should occur in a region where a conductor exists, a current would be induced through the conductor. An induction current consequently flowing through a long-distance transmission line, metallic pipeline or similar structure under the influence of geomagnetic variations may lead to power grid troubles, corroded pipes, and other problems.

A technique called "magnetotellurics" (MT) is also available whereby information on geomagnetic variations is used to estimate

subsurface structures. As a method of measuring subsurface structures, there are two variants of magnetotellurics: measuring an underground resistivity structure by exploiting the skin effect of an AC magnetic field, and estimating a subsurface structure by measuring the local magnetic field anomalies. The first method allows data with high S/N ratios to be collected at times of geomagnetic disturbances because geomagnetic variations are a source of signals, whereas the second method yields data with high S/N ratios in times of quiet geomagnetic conditions because geomagnetic disturbances are also a source of noise. Implementing these methods needs information on geomagnetic variations not for avoiding failures but for effectively conducting MT [7][8].

2.4 Ionospheric storms

Increased auroral activity and ionospheric current in the polar regions following substorms or geomagnetic storms increases the large amount of energy flowing from the magnetosphere into the polar ionosphere by way of particle precipitation, Joule heating, and other processes. This energy heats up the thermosphere to vary atmospheric composition ratios or induce large-scale atmospheric motion, possibly generating an ionospheric storm to vary the critical frequency of the ionosphere and thereby resulting in communication failures [9]. Geomagnetic storms and other disturbances might also heat and expand the thermosphere to significantly alter the attitudes or orbits of artificial satellites at low-earth orbits. The orbital control of low-altitude satellites, satellite reentry control, and similar tasks should therefore benefit from having information about the prediction of geomagnetic disturbances.

3 Monitoring geospace disturbances

Geospace disturbances are manifested as variations of electromagnetic field, plasma particles, and ion composition in geospace. To monitor the particle environment in geospace,

in-situ observations are necessary. However, a multi-point observation network must be built using multi-satellites, since the coverage of single in-situ observation is limited as single point.

On the contrary, electromagnetic field variations due to currents flowing within the magnetosphere and ionosphere can be monitored by remote sensing from the ground. As monitoring of geospace disturbances, we have not only constructed ground-based observation networks to monitor electromagnetic field variations, but also used information of in-situ plasma particle observation and of upstream solar wind and interplanetary magnetic fields via internet. For details about studies conducted on the monitoring, prediction and impact of ionospheric disturbances among all geospace disturbances, refer to other articles included in this special issue.

3.1 INTERMAGNET

Prior to the mid-1990s when the Internet began its widespread proliferation, collecting observational data in quasi-real time had been very difficult. Information accessible for immediate exchange in those days was limited to local geomagnetic indices or event information expressed in “URSIGRAM codes”, such that the work of deriving such indices of global-scale geomagnetic activity as the Kp, Dst and AE indices using worldwide geomagnetic data would take from days to months.

INTERMAGNET was established as a solution to this problem, facilitating the implementation of a global network for collecting geomagnetic data in quasi-real time. INTERMAGNET was started in the late 1980s with primary organized by the U.K. and the U.S. for maintaining the quality of observational data, standardizing observations, exchanging data promptly, and other related tasks. Among the major Japanese participants were the National Institute of Information and Communications Technology (then the Communications Research Laboratory), the World Data Center for Geomagnetism at Kyoto University, and the Kakioka Magnetic Observatory of

the Japan Meteorological Agency. INTERMAGNET linked geomagnetic observatories at remote locations and data-collecting Global Information Nodes (GINs) by meteorological satellite links to transmit data every 12 minutes and collect one-minute values of the three geomagnetic components in quasi-real time a technological breakthrough at a time when only limited geomagnetic disturbance information as expressed by URSIGRAM codes had been available. In Japan, the Hiraiso Solar-Terrestrial Research Center (now the Hiraiso Solar Observatory) served as a GIN to monitor geomagnetic disturbances and made data derived from INTERMAGNET available for real-time public disclosure [10][11].

In line with the subsequent proliferation of the Internet, geomagnetic data has been made easier to exchange since the early days when INTERMAGNET was inaugurated, with more than 100 observatories now participating in the INTERMAGNET global network (Fig. 1). Despite the occasional coordination with observatory-specific data disclosure policies needed to implement real-time data usage, the formation of a global network capable of observing and monitoring geomagnetic disturbance phenomena, and offering its data for shared use should be of great significance.

Moreover, the scheme of exchanging real-time one-second data has been widely discussed in recent years. Such data should prove beneficial in understanding the current conditions of ULF wave activities that offer clues to estimating the acceleration and loss of radiation belt particles.

3.2 PURAES/RapidMAG

Auroras are a variation of the discharge phenomenon occurring in the solar wind-magnetosphere-ionosphere compound system. The flow of intense ionospheric current driven by auroral activity is known to invoke marked geomagnetic variations in the polar regions. The AE index uses those geomagnetic variations as an indicator of geomagnetic activity in the auroral zone. This index had been worked out by Davis and Sugiura [1966] as an indicator of the intensity of electrojets in the auroral zone [12]. The sum of the amplitudes of the + envelope (AU index) associated with intensity of the eastward ionospheric current and the - envelope (AI index) associated with intensity of the westward ionospheric current, along with geomagnetic data collected at the geomagnetic observation points (AE observatories) being overlaid in reference to the quiet level, is called the Auroral Electrojet (AE)

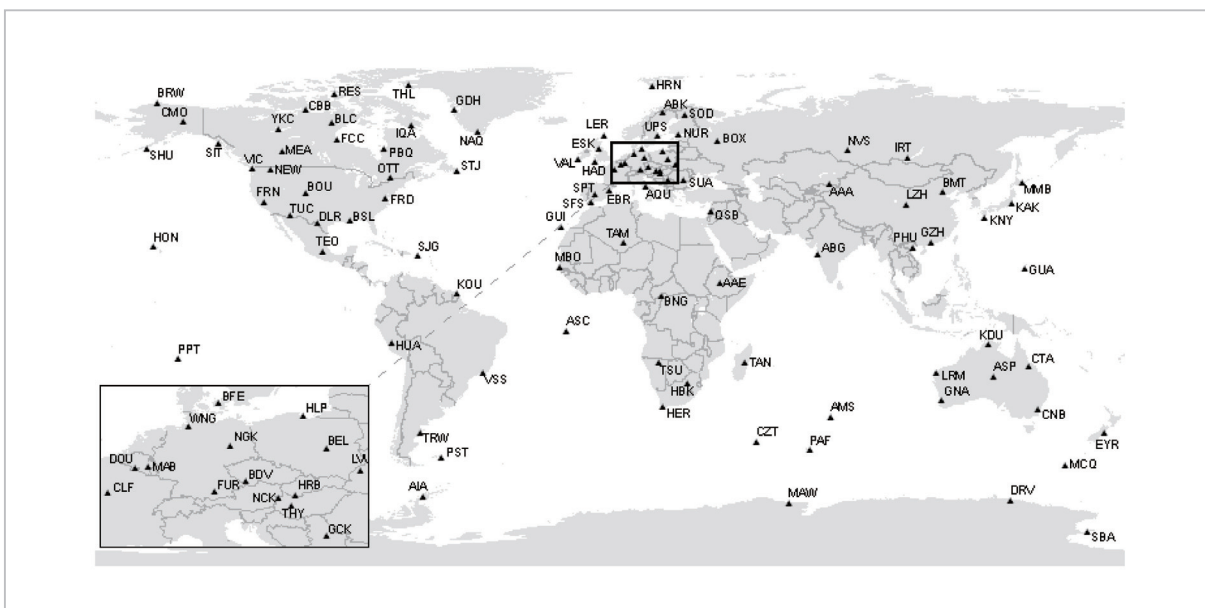


Fig. 1 Worldwide distribution of INTERMAGNET observatories

index. This index is used as an input parameter for models designed to grasp the status of geomagnetic activity in the auroral zone and predict the effects of heating and other conditions of the upper atmosphere as pertaining to auroral activity. For these reasons, the prompt calculation and publication of the AE index has been widely pursued.

Among the AE observatories located in the auroral zone, however, those in the Russian region had used outdated magnetometers

until the mid-1990s that not only yielded data of poor quality but also inhibited the prompt exchange of data (Fig. 2). Therefore, Japan (NICT, World Data Center for Geomagnetism, Kyoto University), the U.S. (Applied Physics Laboratory, Geophysical Institute), and Russia (Arctic and Antarctic Research Institute, Institute of Geospheres Dynamics) worked together to launch a project known as PURAES (Project for Upgrading Russian AE Stations) and its successor RapidMAG (Russian auroral and polar ionospheric disturbance MAGnetometers), in order to promptly collect and disseminate geomagnetic data collected at the AE observatories. NICT is responsible for the portion of the project handling the transmission of data by using geostationary satellites [9]. Geomagnetic data collected at the AE observatories is forwarded to the World Data Center for Geomagnetism at Kyoto University, where AE indices are calculated in quasi-real time from the data before the index data is made public through the Web. Our group's website (URL: <http://kogma.nict.go.jp/cgi-bin/qlae.cgi/>) offers clues to viewing and using real-time AE index data by interactively customizing its time width and scale (Fig. 3).

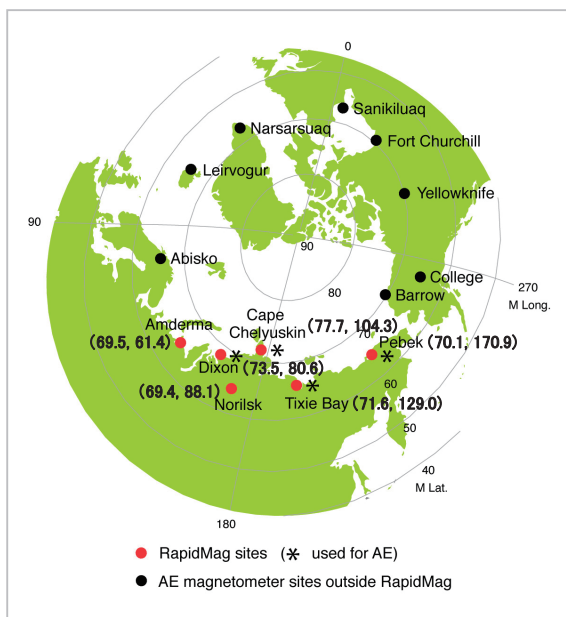


Fig.2 Worldwide distribution of AE observatories

Each red circle denotes the site of an observatory where RapidMAG collects data.

3.3 NICT_MAG

NICT has deployed its own geomagnetic observation network (NICT_MAG) centering on Japan's longitudinal region as part of its space environment monitoring program (NICT_SWM). Figure 4 shows the sites of the observatories. Complementary to INTER-

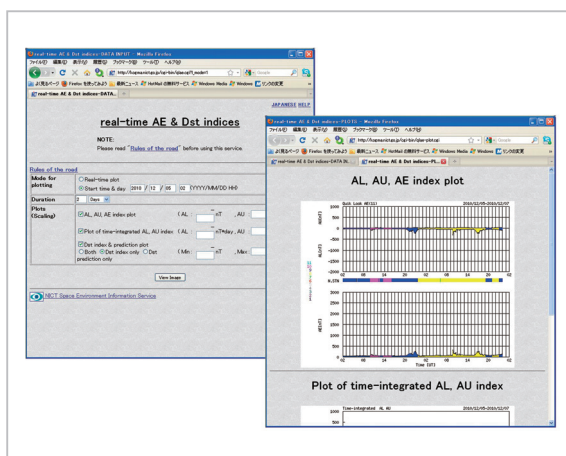


Fig.3 Real-time AE/Dst indices (Web page entry window (left) and plotting window (right))

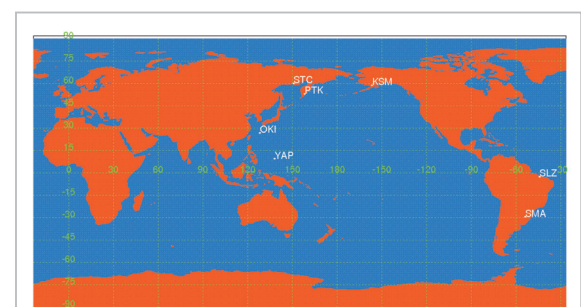


Fig.4 Distribution of observatories in NICT's geomagnetic observation network

MAGNET and RapidMAG, this network collects one-minute, quasi-real-time values the same way. The practical application using the one-minute real-time data are also being studied.

Geomagnetic data collected in quasi-real time can not only be displayed in real time in the form of an online database but may also be plotted to meet interactively customized conditions for date and time, period, scale and other factors [13]. Table 1 lists the observatories where NICT is collecting data in quasi-real time.

3.4 SuperDARN HF radar network

Because geomagnetic variations are produced from variations in the current system in geospace, relevant information aids in estimating current variations in the ionosphere and magnetosphere. Geomagnetic information alone, however, is inadequate for accurately estimating the amount of energy flowing into the polar regions via the current system. Electric field or ionospheric conductivity information is also needed. HF radars provide a tool for measuring a broad range of electric fields. HF radars transmit radio waves in the HF

Table 1 Observatories where NICT collects data in quasi-real time

Location	Obs. Code	Geographic Latitude	Geographic Longitude	Geomag. Latitude	Geomag. Longitude	Partnering institute
INTERMAGNET						
Furstenfeldbruck (Germany)	FUR	48.17	11.28	48.33	94.73	LMU
Tihany (Hungary)	THY	46.90	17.89	45.96	100.60	ELGI
Memambetsu (Japan)	MMB	43.90	144.20	35.62	211.75	JMA
Kakioka (Japan)	KAK	36.23	140.18	27.64	209.20	JMA
Guam (USA)	GUA	13.59	144.87	5.56	216.08	USGS
Hermanus (South Africa)	HER	-34.43	19.23	-34.09	84.63	HMO
RapidMAG						
Dixon (Russia)	DIK	73.50	80.60	64.22	162.64	AARI, etc.
Norilsk (Russia)	NOK	69.80	88.13	60.21	166.48	AARI, etc.
Cape Chelyuskin (Russia)	CCS	77.72	104.28	67.75	178.03	AARI, etc.
Tixie Bay (Russia)	TIK	71.58	129.00	62.05	194.12	AARI, etc.
Peveck (Russia)	PBK	70.09	170.93	64.07	224.01	AARI, etc.
NICT_MAG						
King Salmon (USA)	KSM	58.68	203.35	58.39	259.11	GI
Magadan (Russia)	STC	59.97	150.86	52.12	213.82	IKIR
St.Paratunka (Russia)	PTK	52.94	158.25	46.01	222.00	IKIR
Okinawa (Japan)	OKI	26.75	128.22	17.35	199.07	UR
Yap (FSM)	YAP	9.49	138.09	0.84	209.86	NOAA
Sao Luis (Brazil)	SLZ	-2.60	315.78	6.22	28.15	INPE
Santa Maria (Brazil)	SMA	-29.45	306.17	-19.93	16.99	INPE

LMU: Ludwig-Maximilians-University Munich

ELGI: Eötvös Loránd Geophysical Institute

JMA: Japan Meteorological Agency

USGS: U.S. Geological Survey

HMO: Hermanus Magnetic Observatory

AARI: Arctic and Antarctic Research Institute

GI: Geophysical Institute, University of Alaska

IKIR: Institute of Cosmophysical Researches and Radio Wave Propagation

UR: University of the Ryukyus

NOAA: National Oceanic and Atmospheric Administration

INPE: National Institute for Space Research

band in an oblique upward direction from the ground, and then receive echoes returning from field-aligned ionospheric irregularities as the object of scattering or elsewhere, thereby estimating the velocity of plasma in the ionosphere from the amount of Doppler shift. Once the plasma velocity is estimated, then the amount of electric fields (electric charge) can be estimated from an $E \times B$ drift. Whether echoes are returned depend on whether irregularities meeting the reflecting conditions have occurred in the ionosphere, but HF radars still offer the key advantage of allowing the plasma velocity and electric fields to be derived in the line-of-sight direction in two dimensions, as compared to one-dimensional geomagnetic observations. Under these circumstances, research institutions in various countries including the U.K., France, the U.S., Japan

and South Africa have teamed up to build a network of HF radars called SuperDARN (Super Dual Auroral Radar Network) in the Arctic and Antarctic regions. SuperDARN allows us to gain a two-dimensional insight into the status of plasma convection and electric field distributions in the polar regions. It should be noted, however, that the availability or non-availability of electric field information depends on whether irregularities occurred in the ionosphere satisfy the orthogonal condition for reflecting HF radio waves. NICT maintains an HF radar in King Salmon, Alaska, in order to monitor the status of ionospheric convection flow and electric fields in Japan's longitudinal polar region of eastern Siberia [14] (Figs. 5 and 6).

4 Approaches to predicting geospace disturbances

To predict space weather phenomena, various kinds of methods are considered so far. These methods can be broadly grouped into numeric prediction models (numeric simulations) and empirical models. Numeric prediction models calculate and predict a phenomenon according to physical primitive equations, and promise objective and reliable results based on initial values, given all the physical process and parameters relevant to such prediction, and necessary computer capabilities. Numerical prediction models, however, have a long way to go before reaching a state of practical usefulness due to their ongoing development, with their physical processes yet to be elucidated. For information about the approaches being taken to realize numeric simulations at NICT, refer to another paper [15].

There are many diverse empirical models, ranging from those built to reflect a contextual physical process at the hypothetical level to those that simply build on correlations. These models vary in reliability, but may be better suited for practical use because they derive results with relative ease from input parameters. We have been working on an empirical

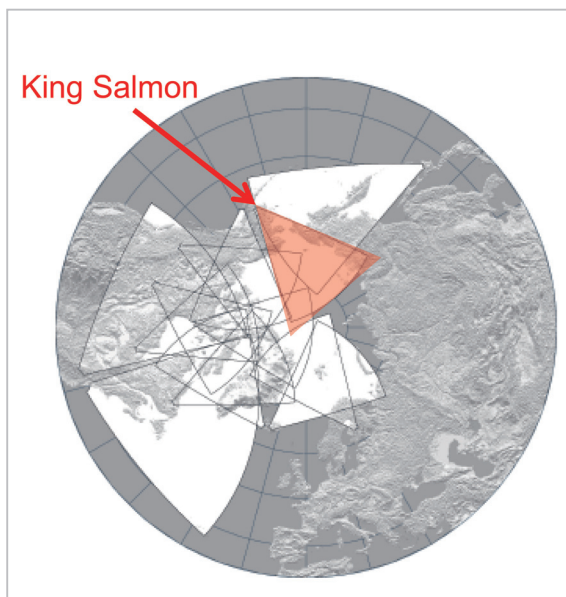


Fig.5 Field observations of SuperDARN in the Northern Hemisphere. The region marked red is the field of view of the King Salmon radar.



Fig.6 Picture of the radar site

prediction model for a geomagnetic index to predict geomagnetic disturbances for use in implementing forecasting services. Since geomagnetic disturbances are the most fundamental of all geospace disturbances, this geomagnetic index should also offer high universal value due to its adaptability as an input parameter to other empirical models (such as those for variations in radiation belt particles).

Various coupling equations using solar wind input parameters have been conceived to date in order to suit a model for predicting geomagnetic indices. Most of these equations assume constant solar wind-magnetosphere coupling efficiency. However, a model that builds on assumed constant coupling efficiency does not explain the seasonal dependence (Equatorial/McIntosh Effect) of geomagnetic variations associated with changes in the inclination of the earth's rotational axis. It has been pointed out that the consideration of seasonal changes in coupling efficiency is a key to solve this problem. However, we did not have enough physical explanations of what causes this effect.

In the meantime, studies conducted over the past 10 years have revealed that plasma convection (polar cap potential) in the magnetosphere peaks without growing at a linear rate [16]. According to one explanation of this characteristic, the regional current system that drives plasma convection grows so that the magnetic field forged by the regional current system deforms the geometry of the magnetosphere by itself, and thus adversely affects the efficiency of interaction between the solar wind and magnetosphere [17]. Relational expressions between the solar wind electric field and the polar cap potential based on this concept are given below.

$$\Phi_{PC} = 57.6 E_m P_{SW}^{1/3} / (P_{SW}^{1/2} + 0.0125 \zeta \Sigma_P E_m) \quad (1)$$

$$\zeta = 4.45 - 1.08 \log \Sigma_P \quad (2)$$

where, Φ_{PC} denotes the polar cap potential, E_m the "merging electric field" expressed by $E_m = V_{SW} B_T \sin^2 (\theta / 2)$ [18], V_{SW} the solar wind velocity, B_T the magnetic field magni-

tude of the YZ plane (with the line interconnecting the sun and earth taken as X), θ the angle relative to north as being 0 degrees, P_{SW} the dynamic pressure, ζ a geometric factor, and Σ_P the Pedersen conductivity.

Because the intensity of the region 1 current system equals the product of the polar cap potential multiplied by the polar cap ionospheric conductivity, the region 1 current system is boosted by increased conductivity, as well as the growing electric field, resulting in the suppressed growth of plasma convection. Given the fact that one region 1 current system exists in the Northern Hemisphere and one in the Southern Hemisphere, previous studies have shown that the degree of growth of the polar cap potential depends on the polar cap ionospheric conductivity (i.e., sum of conductivities in the polar regions above the North and South collected geomagnetic poles [19]). This means that the interaction efficiency of the solar wind-magnetosphere-ionosphere compound system varies as a function of the sum of polar cap conductivity in both hemisphere. We used the am index (an indicator of global geomagnetic activity) and the Km index (an indicator of its logarithmic scale) to probe into the characteristic changes in the interaction efficiency of the solar wind-magnetosphere-ionosphere compound system, and then developed an empirical model that relies on this concept. The use of the am and Km indices offers the advantage of eliminating artificial seasonal changes by reducing biased distributions of the observatories used to derive those indices. Care should be exercised in using the Kp index for statistical purposes, because it is subject to artificial daily and seasonal dependences due to the biased distributions of observatories used to work out the index.

Figure 7 plots the relation between geomagnetic activity and the solar wind electric field as a NetSZA function for each value of the Km index. NetSZA is the sum of the solar zenith angles of the North and South collected geomagnetic poles ($\cos \chi_{NP} + \cos \chi_{SP}$), and a parameter proportional to the sum of conduc-

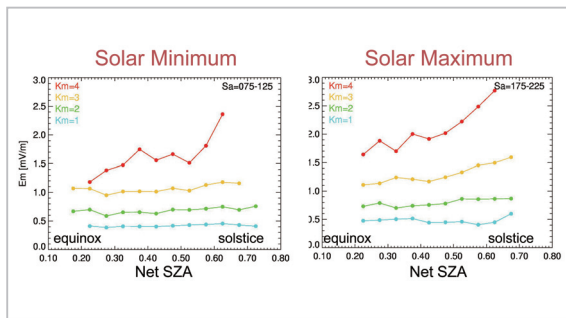


Fig.7 Magnitude of the solar wind electric field needed for geomagnetic activity plotted as a NetSZA function for each value of the Km index (left: solar minimum, right: solar maximum)

tivities in the polar regions above the North and South collected geomagnetic poles as described later. The value of NetSZA is minimized during the spring and autumn equinoxes, and maximized during the summer and winter solstices. The left panel shows the solar minimum (F10.7 index greater than or equal to 75, but less than 125); the right panel shows the solar maximum (F10.7 index greater than or equal to 175, but not more than 225).

In the left panel, the Km index rises to 3 or 4 even in the presence of a weak interplanetary magnetic field when the value of NetSZA is small, but a stronger interplanetary magnetic field would be needed to boost the Km index to 3 or 4 when the value of NetSZA is large. These basic characteristics also hold true in the right panel. A comparison of the left and right panels shows that a stronger electric field is needed to attain the same level of geomagnetic activity during the solar maximum. It has thus been determined that the lower or higher the polar cap potential, the higher or lower the interaction efficiency of the solar wind-magnetosphere-ionosphere compound system. Moreover, the sum of conductivities in the polar regions above the North and South collected geomagnetic poles are minimized during spring and autumn equinoxes and maximized during the summer and winter solstices. This concept may be extended to give a physical explanation of the equinoctial effect. Electrical conductivity also

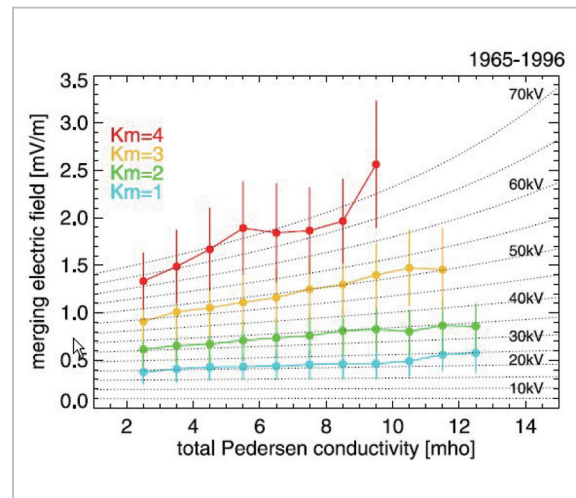


Fig.8 Dependence on conductivity for interaction between the solar wind and magnetosphere

varies as a parameter of solar activity, such that the interaction efficiency is adversely affected during intense solar activity and elevated during periods of quiet solar activity. These effects are in agreement with the results shown in Figure 7. Figure 8 represents the magnitude of the solar wind electric field needed for geomagnetic activity as the sum of conductivities in the polar regions above the North and South collected geomagnetic poles during the solar maximum and solar minimum. Conductivities are expressed in the following equations that were worked out by making unique modifications to a past model [20] that uses the solar zenith angle and F10.7 index as input parameters to calculate conductivity:

$$\Sigma_P = Sa^{0.5} (1.2 \cos \chi + 0.1736) \quad (3)$$

$$\Sigma_{Ptotal} = \Sigma_{PN} + \Sigma_{PS} = Sa^{0.5} (1.2 (\cos \chi_{NP} + \cos \chi_{SP}) + 0.3472) \quad (4)$$

Each background line denotes the value of a polar cap potential predicted from Siscoe. The trends in variations show good agreement, suggesting that variations in the Km and am indices can be represented as a function of polar cap potential.

Based on these findings, an empirical model for predicting the am index has been developed. As stated earlier, the am index

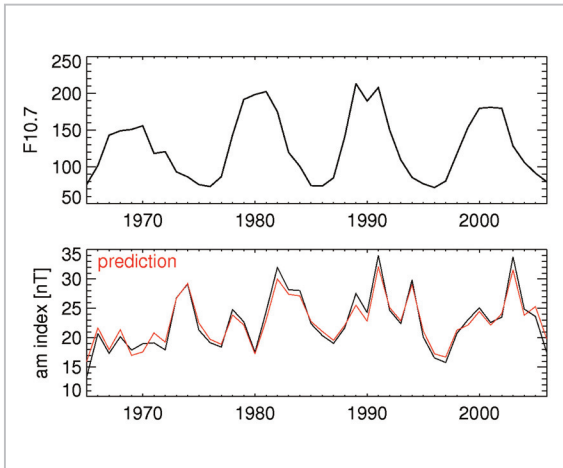


Fig.9 Changes in solar activity and the am index over four solar cycles, and prediction results derived from our empirical model

characteristically depends not only on polar cap potential but also on solar wind dynamic pressure and magnetospheric convection attributed to viscous effects. The solar wind parameters and the am index were analyzed for each of these factors to derive the following three empirical equations:

$$\text{am} (\Phi_{\text{PC}}) = -7.47 - 0.097 \Phi_{\text{PC}} + 0.0079 \Phi_{\text{PC}}^2 \quad (5)$$

$$\text{am} (P_{\text{SW}}) = -1.48 + 7.51 (P_{\text{SW}})^{0.5} \quad (6)$$

$$\text{am} (V_{\text{SW}}) = -0.88 + 0.55 (V_{\text{SW}}/100)^2 \quad (7)$$

The resultant empirical equation of the am index is as follows:

$$\text{am} = -9.83 - 0.097 \Phi_{\text{PC}} + 0.0079 \Phi_{\text{PC}}^2 + 7.51 (P_{\text{SW}})^{0.5} + 0.55 (V_{\text{SW}}/100)^2 \quad (8)$$

Solving Equation (8), along with Equations (1), (2) and (4) given earlier, allow us to calculate the am index from the solar wind velocity, density, magnetic field, F10.7 index, and sum of the solar zenith angles of the North and South collected geomagnetic poles. This

References

- 1 M. Ishii, "Effect of the ionosphere on telecommunications, satellite positioning, and electric navigation," Special issue of this NICT Journal, 3-1-1, 2009.
- 2 T. Nagatsuma, "3.5 Geomagnetic Storms," Journal of Comm. Res. Lab., Vol. 49, No.3. pp. 139–154, 2002.

empirical equation makes it possible to reproduce daily and seasonal geomagnetic changes and solar cycle variations.

Figure 9 compares changes in solar activity and the am geomagnetic index over solar cycles, with the prediction results being derived from our empirical model. Despite variations in solar activity, variations in the am index and its predictions were in good agreement, demonstrating the utility of this empirical model as a tool for the long-term and consistent prediction of geomagnetic activity.

5 Conclusions

Since human beings will expand their sphere of activity toward space environment, the space surrounding the Earth, which we call "geospace", is the unavoidable region for us. Disturbance phenomena occurring in geospace could affect the thermosphere, upper atmosphere, and ground-based social infrastructures. We must therefore monitor geospace disturbances and invest our efforts to predict such phenomena by using models. The scope of prediction should also be expanded from geomagnetic disturbances, the source of other disturbance phenomena, to cover radiation belt disturbances, ionospheric storms, and other disturbances.

Acknowledgements

The International Service of Geomagnetic Indices (ISGI) provided the am and Km indices. Solar wind data was provided from NASA's OMNI2 database. We wish to express our deep appreciation to them.

- 3 M.Nakamura, "Prediction of the plasma environment in the geostationary orbit using the magnetosphere simulation," Special issue of this NICT Journal, 2-2-3, 2009.
- 4 G. Rostoker, "Commentary on the Anik satellite upsets," Report to Telesat Canada, Canadian Network for Space Research Report, January, 1994.
- 5 Research section, Committee of space development, "On the cause of operational anomaly on Advanced Earth Observation Satellite-II (ADEOS-II) and its future countermeasure," The report of space development committee, 2004. (In Japanese)
- 6 H. C. Koons, J. E. Mazur, R. S. Selesnick, J. B. Blake, J. F. Fennell, J. L. Roeder, and P. C. Anderson, "The impact of the space environment on space systems," Proceedings of the 6th Spacecraft Charging Technology Conference, Air Force Research Laboratory, AFRL-VS-TR-20001578, pp. 7–11, 1998.
- 7 Y. Ogawa, "Subsurface Survey using MT method," Chishitsu News, No. 428, pp. 48–54, 1990. (In Japanese)
- 8 Y. Sasai, "Earth electromagnetic exploration — electric underground structure of the Japanese islands," Chikyū, Vol. 10, No. 3, pp. 194–200, 1988.(in Japanese)
- 9 T. Maruyama, "4.4 Ionospheric storm," Wave Summit Course, Science of Space Weather, edited by K. Maruyama, and T. Ondoh, Ohm-sya, 2000.
- 10 H. Ishibashi and K. Nozaki, "Development of the System of INTERMAGNET/HiraisoGIN," Journal of Comm. Res. Lab., Vol. 43, No. 2, pp. 291–299, 1997.
- 11 T. Nagatsuma, H. Ishibashi, and K. Nozaki, "Near real-time on-line geomagnetic field database system," Review of Comm. Res. Lab., Vol. 46, No. 4, pp. 219–228, 2000. (In Japanese)
- 12 T. N. Davis and M. Sugiura, "Auroral electrojet activity index AE and its universal time variations," J. Geophys. Res., Vol. 71, pp. 785–801, 1966.
- 13 M. Kunitake, H. Ishibashi, T. Nagatsuma, T. Kikuchi, and T. Kamei, "3-3 Real-Time Geomagnetic Data Acquisition from Siberia Region and its Application —PURAES Project—," Journal of Comm. Res. Lab., Vol. 49, No. 4, pp. 87–97, 2002.
- 14 T. Kikuchi, K. Hashimoto, M. Shinohara, K. Nozaki, and B. Bristow, "Space weather study using the HF radar in King Salmon, Alaska," Journal of the National Institute of Information and Communications Technology, Vol. 53, Nos.1/2, pp. 113–121, 2007.
- 15 H. Shinagawa, "Significance and importance of the integrated space weather simulation," Special issue of this NICT Journal, 2-3-1, 2009.
- 16 T. Nagatsuma, "Saturation of polar cap potential by intense solar wind electric fields," Geophys. Res. Lett., Vol. 29, No. 10, 1422, doi:10.1029/2001GL014202, 2002.
- 17 G. L., Siscoe, G. M. Erickson, B. U. O. Sonnerup, N. C. Maynard, J. A. Schoendorf, K. D. Siebert, D. R. Weimer, W. W. White, and G. R. Wilson, "Hill model of transpolar potential saturation: Comparisons with MHD simulations," J. Geophys. Res., Vol. 107, No. A6, 1075, doi:10.1029/2001JA000109, 2002.
- 18 J. R. Kan and L. C. Lee, "Energy coupling function and solar windmagnetosphere dynamo," Geophys. Res. Lett., Vol. 6, pp. 577–580, 1979.
- 19 T. Nagatsuma, "Conductivity dependence of cross-polar potential saturation," J. Geophys. Res., Vol. 109, No. A04210, doi:10.1029/2003JA010286, 2004
- 20 J. Moen and A. Brekke, "The solar flux influence on quiet time conductances in the auroral ionosphere," Geophys. Res. Lett., 20, 971–974, 1993.



NAGATSUMA Tsutomu, Dr. Sci.
*Research Manager, Space Environment
Group, Applied Electromagnetic
Research Center*
Solar-Terrestrial Physics